A readily accessible Multifunctional Probe: Simultaneous Recognition of the Cation Zn^{2+} and the Anion F^- via Distinguishable Wavelengths

Li Zeng,‡[a] Jiang-Lin Zhao,‡[b] Lan Mu,[a] Xi Zeng,[a]* Gang Wei,[c]* Carl Redshaw[d] and Zongwen Jin[b]

[a] Key Laboratory of Macrocyclic and Supramolecular Chemistry of Guizhou Province; School of Chemistry and Chemical engineering, Guizhou University, Guiyang 550025, China.
[b] NanoBio Sensing & Manipulation (NBSM), Research Center for Micro/Nano System & Bionic Medicine, Institute of Biomedical & Health Engineering, Shenzhen Institutes of Advanced Technology, Chinese Academy of Sciences, 1068 Xueyuan Avenue, Shenzhen 518055, China.
[c] CSIRO Manufacturing Flagship, PO Box 218, NSW 2070, Australia.
[d] Department of Chemistry, University of Hull, Hull HU6 7RX, U.K.

†Electronic Supplementary Information (ESI) available: Details of ^1H, ^{13}C NMR and MS spectra of probe **1**. See DOI: 10.1039/x0xx00000x

‡Li Zeng and Jiang-Lin Zhao contributed equally to this work. The authors declare no competing financial interest.

The probe **1** was readily prepared via condensation of 8-formyl-7-hydroxy-coumarin and carbonic dihydrazide in a one-step procedure. Probe **1** exhibited high sensitivity and selectivity towards $Zn^{2+}$and F^- through a "turn-on" fluorescence response and/or ratiometric colorimetric response with low detection limits of the order of 10^{-8} M. The complex behaviour was fully investigated by spectral titration, isothermal titration calorimetry, ^1H NMR spectroscopic titration and mass spectrometry. Interestingly, probe **1** not only recognizes the cation Zn^{2+} and the anion F^-, but can also distinguish between these two ions via the max wavelength in their UV-vis spectra (360 nm for **1**-Zn^{2+} *versus* 400 nm for **1**-F^- complex) or their fluorescent spectra (λ_{ex} / λ_{em} = 360 nm/ 454 nm for **1**-Zn^{2+}*versus* λ_{ex} / λ_{em} = 400 nm/ 475 nm for **1**-F^- complex) due to their differing red-shifts. Additionally, probe **1** has been further explored in the detection of Zn^{2+} in living cells.

Introduction

Fluorescent probe assays are one of the most convenient technologies for detecting ions and molecules owing to their high sensitivity, selectivity, rapid response rates and ease of manipulation.[1] Together with their capacity for real-time imaging, these attributes have led to their wide adoption in the detection of biologically relevant ions.[2] A desirable fluorescent probe should not only be easily obtained, but should also allow for the simultaneously detection of both cations and anions with high sensitivity and selectivity. However, most reported probes are capable of only single target detection. Indeed, there are only a limited number of probes which satisfy such requirements, but most of these probes are very difficult to prepare.[3]

Herein, we introduce a facile one step synthesis of a multi-functional, ratiometric colorimetric/fluorescent probe (**1**), which is derived from the condensation reaction of 7-hydroxy-8-aldehyde-coumarin and carbohydrazide. Probe **1** not only exhibits high selectivity for the Zn^{2+} cation, but also high selectivity for F^- anions over a number of other cations and

anions tested herein with distinct colour changes. Furthermore, the response signal for the addition of Zn^{2+} *versus* F^- is easily distinguishable. This selective detection is the result of the 40 nm of wavelength differences observed in the UV-vis absorption spectra upon addition of the Zn^{2+} cation *versus* the F^- anion. Hence, using **1** it is not only possible to detect Zn^{2+} cations and F^- anions, but it can also distinguish between these two ions.

Among the various transition metal ions, zinc is the second most abundant transition metal in the human body. It plays a versatile role in a number of biological processes such as in the regulation of metalloenzymes, DNA binding and/or recognition, structural cofactors, neural signal transmission, as a catalytic center in many other processes.[4] Many Zn^{2+} fluorescent probes have been reported, which exhibited selectivity and sensitivity over other biologically essential metal ions over specific concentration ranges.[5] Although there are many Zn^{2+} probes, they are mostly for single target detection, and it is still a challenge to develop multi-functional and multi-analyte responsive probes.

On the other hand, anions are ubiquitous and have major roles in a wide range of chemical, biological and environmental processes. The importance of anions has led to ongoing efforts in the development of sensors capable of selective recognition and sensing of anions.[6] Among these efforts, fluoride recognition has attracted substantial interest not only because of its unique properties but also its importance in our daily life.[7] Thus, the sensing of F^- has become a major focus and some excellent progress has recently been published.[8] In this paper, a multi-functional probe **1** is reported which possesses the ability to detect and distinguish Zn^{2+} and F^-.

Results and discussion

Synthesis

Probe **1** was obtained by the convenient condensation reaction of 8-formyl-7-hydroxy-coumarin and carbonic dihydrazide in a one-

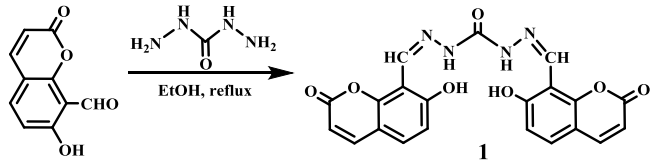

Scheme 1 The synthetic route to probe **1**.

step process (Scheme 1). Its structure was elucidated by IR, ^{1}H NMR, ^{13}C NMR spectroscopy and mass spectrometry. The proton signal of the precursor aldehyde group had disappeared, whilst a new singlet appeared at about 8.99 ppm, which was attributed to the CH=N protons of the Schiff base skeleton (for details, see the Supporting Information, Fig. S1-S3).

Optical response of probe 1 to Zn^{2+}

Fluorescence and UV-vis absorption spectroscopy were employed herein to investigate the recognition properties of probe **1**. In DMF/H_2O (2/3, v/v) solution, among the various tested metal cations Li^{+}, Na^{+}, K^{+}, Ag^{+}, Zn^{2+}, Mg^{2+}, Ca^{2+}, Ba^{2+}, Sr^{2+}, Hg^{2+}, Co^{2+}, Ni^{2+}, Cu^{2+}, Pb^{2+}, Cd^{2+}, Al^{3+}, Cr^{3+} and Fe^{3+}, probe **1** exhibited highly selective fluorescence enhancement in the presence of Zn^{2+} (the quantum yield Φ = 0.38 *versus* quinine sulfate as reference material, Φ = 0.56), whilst no significant fluorescence intensity changes were observed in the presence of any of the other metal ions (Fig. 1a). The fluorescence enhancement of probe **1** in the presence of Zn^{2+} could be ascribed to the formation of a chelate complex (rigid system) between probe **1** and the Zn^{2+} ion, leading to the chelation-enhanced fluorescence (CHEF) effect.[9] Meanwhile, the chelate effect also resulting in the inhibition of the C=N isomerization process and decreased non-radiative decay of the excited-state.[10] Fluorescence titration experiments revealed the detail complexation information for the process of probe **1** complexed with the Zn^{2+} (Fig. 1b). As expected, when the concentration of Zn^{2+} was gradually increased from 0 to 4 equiv., the corresponding fluorescence intensity of probe **1** was gradually enhanced. The complex reached equilibrium with 1 equiv. Zn^{2+}, as shown in the molar ratio inset. The 1:1 complex stoichiometry was further confirmed by a Job's plot (Fig. 1b, inset).

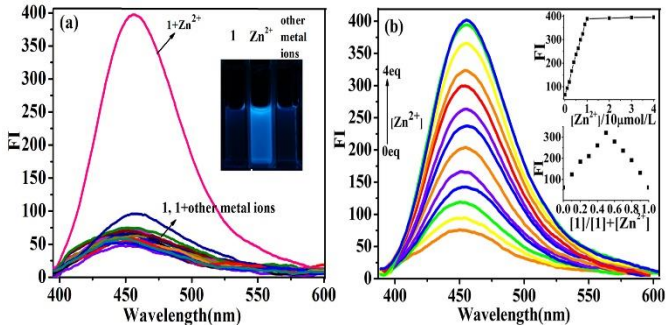

Fig. 1 (a) Fluorescence spectra of probe **1** (10 μM, DMF/H_2O, 2/3, v/v) with 20 eq. of different metal ions (inset shows the colour change of probe **1** in the absence and the presence of Zn^{2+} under UV-vis light.); (b) Fluorescence spectral titration (inset shows variation of fluorescence intensity against the number of equivalents of Zn^{2+} and Job's plot data.). λ_{ex} / λ_{em} = 360 nm/ 454 nm.

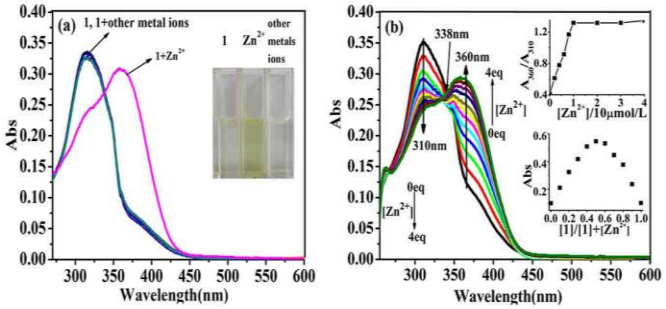

Fig. 2 (a) Absorption spectra of probe **1** (10 μM, DMF/H_2O, 2/3, v/v) with 20 equiv. of different metal ions. (b) Absorption spectral titrations of probe **1** (10 μM, DMF/H_2O, 2/3, v/v) with Zn^{2+}. (a): inset shows the colour change of probe **1** in the absence and the presence of Zn^{2+} under day light; (b): inset shows variation of ratio absorbance against the number of equivalents of Zn^{2+} and Job's plot data. $A_{360\ nm}/ A_{310\ nm}$.

Interestingly, the UV-vis absorption spectra of probe **1** exhibited a more remarkable phenomenon for the Zn^{2+} recognition. A dramatic red-shift (shifted from 310 nm to 360 nm) was observed in the presence of Zn^{2+} without any interference. It strongly suggested that Zn^{2+} ions can be readily and selectivity recognized by probe **1** (Fig. 2a). Additionally, we can directly distinguish Zn^{2+} ion from various cations by the naked eye based on obvious colour changes (from colorless to bright yellow (Fig. 2a, inset). Furthermore, the UV-vis absorption titration experiment revealed a ratiometric behaviour with the formation of a new band at 360 nm and a decrease in the absorption band at 310 nm upon addition of Zn^{2+} (Fig. 2b); isosbestic points appear at 338 nm. It is well-known that ratiometric response probes are better than any of other type of probes given their built-in correction for environmental effects and self-correcting capability.[11] All of these results are clear evidence that probe **1** could serve as a probe for the detection of Zn^{2+}. Molar ratio and Job's plot analysis revealed a 1:1 stoichiometry (Fig. 2b, inset) for the complexation, which was further confirmed by MALDI-TOF mass spectrometry (Fig. S5). A mass peak at $^m/_z$ 499.545 (calculated value 499.409) was observed which corresponded to [**1**+Zn]$^+$, strongly suggestive of the formation of a 1:1 complex, i.e. **1**-Zn^{2+}.

Optical response of probe 1 to F^-

In order to fully investigate the recognition properties of probe **1**, the interaction of probe **1** (10 μM) towards anions were also investigated by fluorescence and UV-vis absorption spectroscopy in DMF solution. It was observed that there were no obvious changes in the fluorescence emission spectra upon addition of 20 equiv. of Cl^-, Br^-, I^-, NO_3^-, HSO_4^-, $H_2PO_4^-$, PF_6^- and ClO_4^- except for F^- (Fig. 3a). The addition of F^- induced an acutely fluorescence enhancement (Φ = 0.39 *versus* quinine sulfate as reference material, Φ = 0.56) with a red shift from 440 nm to 475 nm which was attributed to the formation of a **1**-F^- complex. The colour of the solution changed from blue to a blue/green colour under ultraviolet light (Fig. 3a, inset). Most noteworthy, a dramatic red-shift (from 310 nm to 400 nm) for F^- was observed in the UV-vis absorption spectra (Fig. 3b).

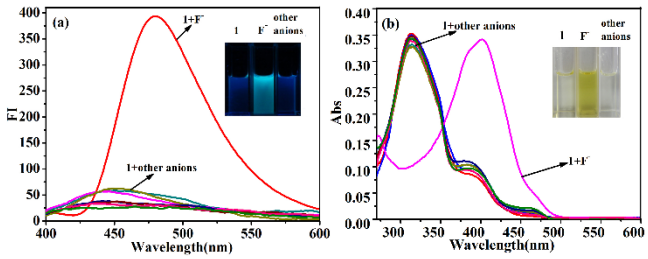

Fig. 3 Fluorescence (a) and absorption (b) spectra of probe **1** (10 μM, DMF) with different anions (200 μM). Inset shows the colour change of probe **1** in the absence and the presence of F^- under UV-vis light (a), under day light (b). Anions: F^-, Cl^-, Br^-, I^-, NO_3^-, HSO_4^-, $H_2PO_4^-$, PF_6^-, ClO_4^-. λ_{ex} = 400 nm.

Distinct colour changes (from colourless to deep yellow) were observed in the presence of F^-, and these could be visualized by the naked eye for detecting F^- *versus* the various other anions screened herein using probe **1** (Fig. 3b, inset). These observations strongly suggested that probe **1** is also an excellent probe for the detection of F^-.

In order to obtain more detailed complexation information for probe **1** with F^-, fluorescence and UV-vis absorption titration experiments were also carried out. As expected, when the concentration of F^- was gradually increased from 0 to 4 equiv., the fluorescence intensity of probe **1** was gradually enhanced by about 7.4-fold in the fluorescence spectra (Fig. 4a). On the other hand, the UV-vis absorption titration experiments revealed a ratiometric

behaviour with the formation of a new band at 400 nm for F^-, and a decrease in the absorption band at 310 nm upon addition of F^- (Fig. 4b). This was also attributed to the formation of multiple hydrogen bonding involving the two phenolic-OH groups and two amide-NH groups. This binding interaction locks the C=N bond of **1** in place preventing its rapid isomerization and switching the fluorescence "on" which also seems to affect the intramolecular charge transfer (ICT) within the probe resulting in a red shift and a fluorescence colour change from non-fluorescence to blue/green. As mentioned previously, the unique ratiometric behaviour ($A_{310\ nm}/A_{400\ nm}$ for **1**-F^-), can provide a built-in correction for the environmental effect.

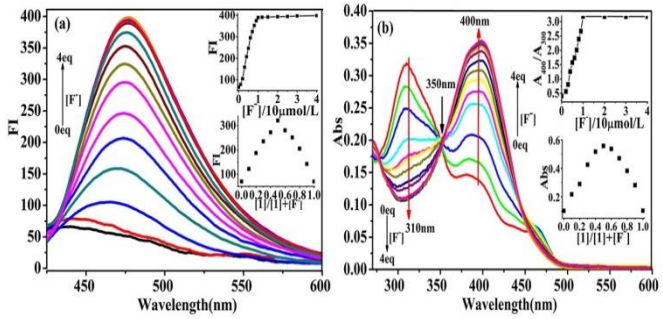

Fig. 4 Fluorescence (a) and absorption (b) spectral titrations of **1** (10 μM, DMF) with F^-. Inset shows variation of fluorescence intensity (a) and ratio absorbance (b) against the number of equivalents of F^- and Job's plot data. λ_{ex} / λ_{em} = 400 nm/ 475 nm, $A_{400\ nm}/A_{310\ nm}$.

Table 1 Complex stability constant (KS), enthalpy (ΔH°) and entropy change (TΔS°) for the complexation of probe **1** with Zn^{2+} and F^- in DMF solution at 293.15 K

Complex	*n*	K_S /(L·M^{-1})	Δ*H*° /(kJ·M^{-1})	*Δ*S*° /(J·M^{-1})
1-Zn^{2+}	1.00±0.024	(1.19±0.03)×10^4	-36.10±2.11	220.3
1-F^-	1.28±0.021	(5.24±0.04)×10^4	-54.41±3.21	275.9

Hence, probe **1** can also act as an excellent ratiometric probe for F^- due to the self-correcting capability. A 1:1 stoichiometry was confirmed by molar ratio and Job's plot (Fig. 4 inset).

Additionally, isothermal titration calorimetry (ITC) was employed here as it is a useful method for monitoring host-guest interactions.[12] In contrast to the experimental conditions for the preparation of cations/receptors complexes, ITC can still provide useful information on the interaction between guest cations and host receptors solutions. As shown in Figure S6a, a representative titration curve can be obtained from an ITC experiment which revealed an abrupt transition point when the molar ratio of Zn^{2+} and probe **1** reached 1, indicating the formation of a 1:1 complex of Zn^{2+} ion with probe **1**. Similar features were observed in the case of the **1**-F^- complexes (Fig. S6b). Furthermore, the free energy *Δ*G*° < 0 [-(95.68 ± 2.13) kJ·M^{-1} for **1**-Zn^{2+}complexs and -(138.49 ± 5.12) kJ·M^{-1} for **1**-F^- complexes] indicated that the binding processes are spontaneous. The association constants (K_a) were determined to be (1.19 ± 0.03) × 10^4 M^{-1} for **1**-Zn^{2+} and (5.24 ± 0.04) × 10^4 M^{-1} for **1**-F^- by using the ITC method, respectively (Table 1). All of these results are clear evidence that probe **1** is an excellent probe for both Zn^{2+} and F^- ions.

To further investigate the practical applicability of probe **1** (10 μM) as a Zn^{2+} ion selective fluorescent probe, competitive experiments were carried out in the presence of Zn^{2+} (20 eq.) mixed with Li^+, Na^+, K^+, Mg^{2+}, Ca^{2+}, Ba^{2+}, Sr^{2+}, Co^{2+}, Ni^{2+}, Pb^{2+}, Cd^{2+}, Ag^+, Hg^{2+}, Cu^{2+}, Fe^{3+}, Al^{3+} and Cr^{3+} (20 eq.) in DMF/H_2O, (2/3, v/v) solution. As shown in Fig. S7, no significant interference to the selective response of probe **1** to Zn^{2+} was observed in the presence of any of the other metal ions employed herein when using either the UV-vis and fluorescence method. Similarly, competitive anion experiments were also carried out in the presence of F^- mixed with 20 equiv. of coexisting anions Cl^-, Br^-, I^-, HSO_4^-, NO_3^-, ClO_4^-, PF_6^- and $H_2PO_4^-$ in DMF solution. As shown in Fig. S8, no obvious interference in the detection of

Table 2 Analysis parameters for **1** and detection of Zn^{2+} and F^-.

Method	The linear range of the calibration curve (μM)	Correlation coefficient	Limits of detection (×10^{-8} M)

Fluorescence	0.1 ~ 12 (Zn^{2+})	0.9973 (n=11)	3.4
	0.1 ~ 11 (F^-)	0.9809 (n=11)	2.9
Absorption	0.2 ~ 12 (Zn^{2+})	0.9925 (n=11)	16
	0.4 ~ 10 (F^-)	0.9850 (n=11)	36

F^- with probe **1** was observed in the presence of other competitive anions. Accordingly, these observations strongly suggested that probe **1** can be used as a selective probe for Zn^{2+} and F^- in the presence of the above mentioned ions for real life applications. Under the optimal conditions, the detection of linear relationships and limits of detection (LOD = 3σ /slope) of probe **1** for Zn^{2+} and F^- are summarized in Table 2. The LOD of probe **1** towards the cation Zn^{2+}, and the anions F^- were of the order of 10^{-8} M by fluorescence or 10^{-7} M by the colorimetric method, which are far below most previously reported systems (Table S1).[3b, 8a, 15]

Cell imaging study

The capability of probe **1** to detect Zn^{2+} within living cells was investigated by fluorescence imaging on a fluorescence microscope, and the optical window at the blue channel was chosen as a signal output. Incubation of PC3 cells with 10 μM of probe **1** for 30 min at 37 °C gave almost no intracellular fluorescence as monitored in the bright-field image (Fig. 6a and 6e) and in the fluorescence image (Fig. 6b and 6f) by fluorescence microscopy. The incubated cells were then treated with 50 μM of Zn^{2+} for 30 min, whereupon a remarkable intracellular fluorescence was observed (Fig. 6c and 6g). However, the fluorescence can be quenched in the presence of membrane permeable Zn^{2+} chelators, such as, 100 μM TPEN (Fig. 6d) or 70 μM EDTA (Fig. 6h) over 45 min. This "on-off" fluorescence behaviour in living cells was attributed to the strong scavenging action of TPEN (or EDTA) toward Zn^{2+}. It unambiguously confirmed that the blue fluorescence was induced by the response of probe **1** towards intracellular Zn^{2+}. This result suggested that probe **1** can penetrate the cell membrane in a short time and can monitor intracellular Zn^{2+} in PC3 cells by *in vitro* imaging and also potentially by *in vivo* methods.

Unfortunately, similar methods were unsuccessful when applied to the monitoring of F^- anions in living cells due to the presence of water, which resulted acute florescence quenching for the **1**-F^- complex.

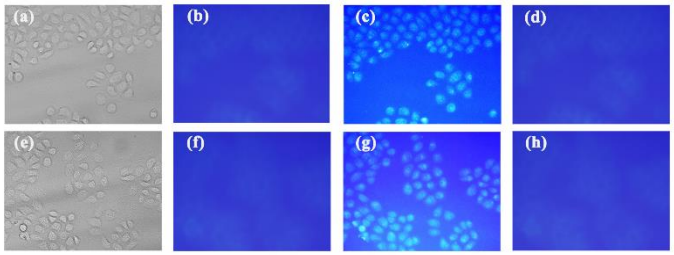

Fig. 6 Fluorescence images of PC3 cells: (a) and (e) bright-field image of cells after incubation with probe **1** (10 μM); (b) fluorescence image of (a); (f) fluorescence image of (e); (c) and (g) blue fluorescence image of probe **1** (10 μM) treated cells after incubation with Zn^{2+} (50 μM) solution; (d) fluorescence image of probe **1** and Zn^{2+} solution treated cells which are the same as (c) after further incubation with TPEN (100 μM); (h) fluorescence image of probe **1** and Zn^{2+} solution treated cells which are the same as (g) after further incubation with EDTA (70 μM)

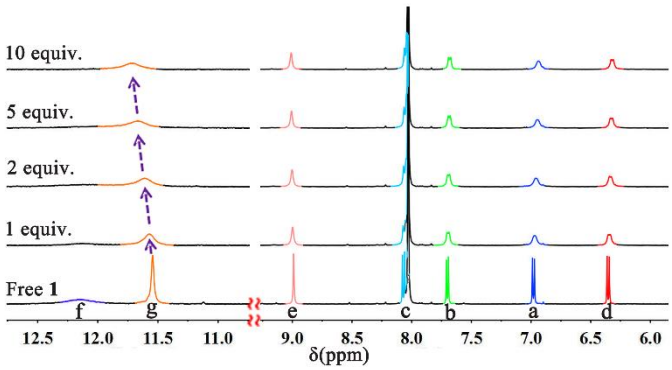

Fig. 7 Partial ^{1}H NMR spectra of probe **1** (5.0 mM) and increasing concentrations of Zn^{2+} in DMF-d_7 at 298K.

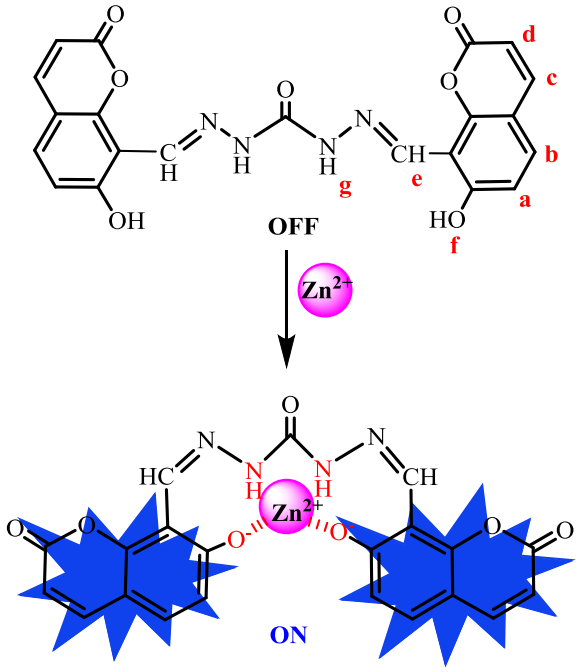

Scheme 2. Plausible binding model for the **1**-Zn^{2+} complex.

The recognition mechanism of probe 1 towards ions

To further understand the recognition mechanism between probe **1** and Zn^{2+}, ^{1}H NMR titration studies were initiated in DMF-d_7 (Fig. 7). When the concentration of Zn^{2+} was gradually increased, the proton signal of the hydroxyl group (*OH*, H_f) disappeared which may be attributed to deprotonation of the hydroxyl forming $O^-\cdots Zn^{2+}\cdots O^-$ interactions for complexation. Whilst the gradually lower field shift and broadening of the amide proton signal (*NH*, H_g) indicated that the amide group was affected by the complexation with Zn^{2+}. In other words, the amide moiety surrounds the Zn^{2+} to assistant the complexation process. However, there was no appreciable proton signal change for the coumarin moieties and the –N=CH protons (H_a ~ H_e). Thus, we propose the possible binding model for **1**-Zn^{2+} as shown in scheme 2.

^{1}H NMR titrations experiments were also carried out to investigate the F^- anion binding properties of probe **1** in

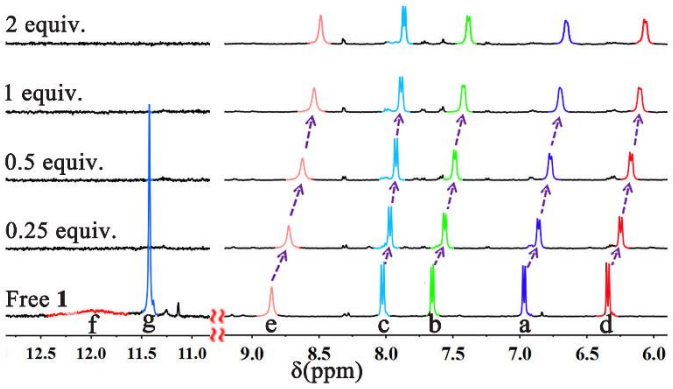

Fig. 8 Partial ^{1}H NMR spectra of probe **1** (5.0 mM) and increasing concentrations of F^- in DMSO-d_6 at 298K.
Scheme 3 Plausible binding model of the **1**-F^- complexes.

DMSO-d_6. The proton hydroxyl *OH* signal (H_f, 11.98 ppm) and the amide *NH* proton (H_g, 11.12 ppm) of probe **1** disappeared when only 0.25 equiv. of F^- was added to the solution (Fig. 8). However, no characteristic peak was observed in the region of ~16.0 ppm due to the formation of an H-F^- complex even on increasing the addition of 2.0 eq. of F^-.[13] These observations suggested that probe **1** complexed with F^- through multiple hydrogen bonds to form a host-guest complex without any deprotonation events. Simultaneously, the –N=CH proton (H_e) and all the aromatic protons of the coumarine moieties (H_a, H_b, H_c, H_d) exhibited a progressive upfield shift which may be attributed the π-π stacking between two coumarine which induced a shielding effect (Fig. 8). Thus, we propose the possible anion complexation mode for probe **1** as in Scheme 3.

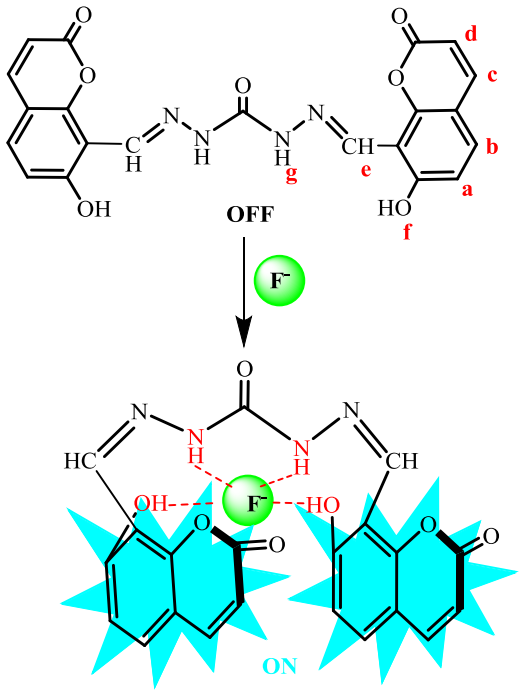

Scheme 3 Plausible binding model of the **1**-F^- complexes.

DMSO-d_6. The proton hydroxyl *OH* signal (H_f, 11.98 ppm) and the amide *NH* proton (H_g, 11.12 ppm) of probe **1** disappeared when only 0.25 equiv. of F^- was added to the solution (Fig. 8). However, no characteristic peak was observed in the region of ~16.0 ppm due to the formation of an H-F^- complex even on increasing the addition of 2.0 eq. of F^-.[13] These observations suggested that probe **1** complexed with F^- through multiple hydrogen bonds to form a host-guest complex without any deprotonation events. Simultaneously, the –N=CH proton (H_e) and all the aromatic protons of the coumarine moieties (H_a, H_b, H_c, H_d) exhibited a progressive upfield shift which may be attributed the π-π stacking between two coumarine which induced a shielding effect (Fig. 8). Thus, we propose the possible anion complexation mode for probe **1** as in Scheme 3.

Conclusions

In summary, a fluorescent and ratiometric colorimetric probe **1** for Zn^{2+} and F^- has been readily prepared in a one-step procedure. Probe **1** exhibits high sensitivity and selectivity for Zn^{2+} and F^- through a "turn-on" fluorescence response over a range of other tested metal ions or anions with detection limits as low as 3.4 $\times 10^{-8}$ M and 2.9$\times 10^{-8}$ M, respectively. Additionally, it also possesses excellent ratiometric behaviour towards Zn^{2+} and F^- which enables **1** to serve as a ratiometric probe. Moreover, we can easily distinguish the cation Zn^{2+} and the anions F^- via their max wavelength in their UV-vis spectra (360 nm for **1**-Zn^{2+} *versus* 400 nm for **1**-F^- complex) or their fluorescent spectra (λ_{ex} / λ_{em} = 360 nm/ 454 nm for **1**-Zn^{2+} *versus* λ_{ex} / λ_{em} = 400 nm/ 475 nm for **1**-F^- complex) which are attributed to the differing red-shifts. The complexation behaviour, mechanism was fully investigated by UV-vis and fluorescent spectral titrations, isothermal titration calorimetry, ^{1}H NMR spectroscopic titrations and mass spectrometry. Furthermore, the utility of probe **1** as a biosensor in living cells (PC3 cells) towards Zn^{2+} ions have been demonstrated. This work provides a promising strategy for the detection of metal ion and anionic species in biological and environmentally relevant systems.

Experimental

Materials and methods

Unless otherwise stated, all reagents used were purchased from commercial sources and were used without further purification. 8-Formyl-7-hydroxy-coumarin was prepared following the reported procedure.[14] The solutions of the metal ions were prepared from their nitrate salts (Aldrich and Alfa Aesar Chemical Co., Ltd.). All the anions used were tetra-*n*-butylammonium salts (Sigma-Aldrich Chemical Co.), and were stored in a desiccator under vacuum containing self-indicating silica. Other chemicals used in this work were of analytical grade and were used without further purification. Double distilled water was used throughout. Fluorescence spectral measurements were performed on a Cary Eclipse fluorescence spectrophotometer (Varian) equipped with a xenon discharge lamp using a 1 cm quartz cell. UV-vis spectra were recorded on a UV-1800 spectrophotometer (Beijing General Instrument Co., China). IR spectra were obtained using a Vertex 70 FT-IR spectrometer (Bruker). ^{1}H and ^{13}C NMR spectra were measured on a WNMR-I 500 MHz NMR spectrometer (Wuhan Institute of Physics and Mathematics, Chinese Academy of Sciences) or a Nova-400 NMR spectrometer (Varian) respectively at room temperature using TMS as an internal standard. ESI-MS spectra were recorded on a Q Exactive spectrometer (Thermo). MALDI-TOF mass spectra were measured on a BIFLEX III ultra-high resolution Fourier transform ion cyclotron resonance (FT-ICR) mass spectrometer (Bruker) with α-cyano-4-hydroxycinnamic acid as matrix. Isothermal titration calorimetry experiments were performed using a Nano ITC (TA); Cell fluorescence imaging was performed using an IX-71 (Olympus) fluorescence inverted phase contrast microscope.

Synthetic of probe 1

A solution of 8-formyl-7-hydroxy-coumarin (600 mg, 3.16 mmol) in dry ethanol (70 mL) was added dropwise to a solution of carbohydrazide (140 mg, 1.58 mmol) in dry ethanol (50 mL). The mixture was heated at reflux for 24 h. The product was collected by filtration and recrystallized from chloroform/methanol (4/1, v/v) and obtained as a milky solid (471 mg, 68.7 %). m.p. > 300 °C; IR (cm^{-1}): 3466, 2929, 2073, 1726, 1610, 1243, 842. ^{1}H NMR (500 MHz, DMF-d_7): δ = 6.35 (d, 2 H, J = 10 Hz), 6.98 (d, 2 H, J = 10 Hz), 7.70 (d, 2 H, J = 10 Hz), 8.07 (d, 2 H, J = 10 Hz), 8.99 (s, 2 H), 11.54 (s, 2 H) and 12.14 (s, 12.14) ppm; ^{13}C NMR (DMF-d_7): 162.1, 160.7, 154.5, 152.4, 145.8, 141.1, 131.7, 114.8, 113.1, 112.5 and 107.4 ppm; HRMS (ESI/TOF-Q) *m/z*: $[M+H]^+$ Calcd for $C_{21}H_{15}N_4O_7$ 435.09407; Found 435.09372.

Spectral measurements

To a 10 mL volumetric flask containing different amounts of ions, the appropriate amounts of the solution of probe **1** were added directly with a micropipette, for Zn^{2+}, then diluted with DMF/H_2O (2/3, v/v) mixed solvent to 10 mL; for F^-, diluted with DMF to 10 mL, then the fluorescence and absorption sensing of the ions was conducted. The fluorescence and UV-vis spectra were measured after addition of ions at room temperature to equilibrium. Fluorescence measurements were carried out with an excitation and emission slit width of 10 nm.

Isothermal titration calorimetry determination (ITC)

The ITC experiment consisted of 35 consecutive injections, each at intervals of 240 s of 7 μL of ion solution (Zn^{2+} and F^- 1 mM) into the micro calorimetric reaction cell (1 mL) charged with a solution of probe **1** (0.1 mM) at 293.15 K with a stirring rate of 300 r/min. DMF solvent was added to the reference cell as a thermal equilibrium reference. The heat of reaction was corrected for the heat of dilution of the ion solution determined in separate experiments. All solutions were degassed prior to the titration experiments by sonication. Computer simulations (curve fitting) were performed using the Nano ITC analyze software.

Cell culture and fluorescence imaging

PC3 cells were grown using a Roswell Park Memorial Institute-1640 supplemented with 10% fetal bovine serum, 100 U/mL penicillin and 100 μg/mL streptomycin at 37 °C and 5% CO_2. One day prior to imaging, the cells were seeded in 6-well flat-bottomed plates. The next day, the cells were incubated with 10 μM of probe **1** for 30 min at 37 °C. Before incubating with 50 μM $Zn(NO_3)_2$ for another 30 min, the cells were rinsed with fresh culture medium three times to remove the remaining sensor, then the fluorescence imaging of intracellular Zn^{2+} was observed under an inverted fluorescence microscope excited with UV light. The fluorescence imaging was observed after treatment of the cells with metal ion chelator, either 100 μM TPEN or 70 μM EDTA for 45 min. The cells when only incubated with 10 μM of probe **1** for 30 min acting as a blank control.

Acknowledgements

This work was supported by the Natural Science Foundation of China (No. 21165006), the "Chun-Hui" Fund of Chinese Ministry of Education (No. Z2015007), Basic Research Program of Shenzhen (NO.

JCYJ20140610151856726), Technology Research Program of Shenzhen (NO. JSGG20141118113131546), China Postdoctoral Science Foundation (NO. 2015M582439) Guangdong Innovative Team Program (NO. 2013S046) and Shenzhen Peacock Plan. The EPRSC are thanked for the financial support (Overseas Travel award to CR).

Notes and references

1 (a) W. Sun, S. G. Guo, C. Hu, J. L. Fan and X. J. Peng, *Chem. Rev.*, 2016, **116**, 7768; (b) Y. J. Chen, S. C. Yang, C. C. Tsai, K. C. Chang, W. H. Chuang, W. L. Chu, V. Kovalev and W. S. Chung, *Chem. Asian J.*, 2015, **10**, 1025; (c) S. Samanta, B. K. Datta, M. Boral, A. Nandan and G. Das, *Analyst*, 2016, **141**, 4388; (d) H. Sui, Y. Wang, Z. Yu, Q. Cong, X. X. Han and B. Zhao, *Talanta*, 2016, **159**, 208; (e) E. Karakus, M. Ucuncu and M. Emrullahoglu, *Anal. Chem.*, 2016, **88**, 1039; (f) Z. J. Zhou, L. Xiao, Y. Xiang, J. Zhou and A. J. Tong, *Anal. Chim. Acta.*, 2015, **889**, 179; (g) E. Galbraith and T. D. James, *Chem. Soc. Rev.*, 2010, **39**, 3831.

2 (a) J. J. Du, M. M. Hu, J. L Fan and X. J. Peng, *Chem. Soc. Rev*., 2012, **41**, 4511; (b) M. Saleem and K. H. Lee, *RSC Adv*., 2015, **5**, 72150; (c) G. R. You, G. J. Park and S. A. Lee, *Sensors and Actuators B*., 2014, **202**, 645; (d) H. Zhu, J. L. Fan and B. Wang, *Chem. Soc. Rev*., 2015, **4**4, 4337; (e) L. E. S. Figueroa, M. E. Moragues and E. Climent, *Chem. Soc. Rev*., 2013, **42**, 3489.

3 (a) T. Ghosh, B. G. Maiya and A. Samanta, *Dalton Trans*., 2006, 795; (b) M. Shellaiah, Y. H. Wu and H. C. Lin, *Analyst.*, 2013, **138**, 2931; (c) M. D. C. González, F. Otón and A. Espinosa, *Org. Biomol. Chem*., 2015, **13**, 1429; (d) C. Bhaumik, S. Das and D. Maity, *Dalton Trans*., 2011, **40**, 11795; (e) S. R. Patil, J. P. Nandre and D. Jadhav, *Dalton Trans*., 2014, **43**, 13299 ; (f) E. J. Song, H. Kim and I. H. Hwang, *Sensor and Actuators B*., 2014, **195**, 36.

4 (a) D. Karak, S. Das and S. Lohar, *Dalton Trans*., 2013, **42**, 6708; (b) C. J. Frederickson, J. Y. Koh and A. I. Bush, *Nat. Rev. Neurosci*., 2005, **6**, 449; (c) P. J. Fraker and L. E. King, *Annu. Rev. Nutr*., 2004, **24**, 277.

5 (a) E. Manandhar, J. H. Broome and J. Myrick, *Chem. Commun*., 2011, **47**, 8796; (b) K. Aich, S. Goswami and S. Das, *RSC Adv*., 2015, **5**, 31189; (c) D. Y. Wu, L. X. Xie and C. L. Zhang, *Dalton Trans*., 2006, 3528.

6 (a) P. A. Gale, *Chem. Soc. Rev*., 2010, **39**, 3746; (b) C. Caltagirone and P. A. Gale, *Chem. Soc. Rev*., 2009, **38**, 520; (c) J. L. Sessler, P. A. Gale and W. S. Cho, Cambridge, 2006; (d) P. D. Beer and P. A. Gale, *Angew. Chem. Int. Ed*., 2001, **40**, 486; (e) D. Ghosh, S. Rhodes and K. Hawkins, *New J. Chem*., 2015, **39**, 295; (f) T. D. Ashton, K. A. Jolliffe and M. Frederick, *Chem. Soc. Rev*., 2015, **44**, 4547.

7 (a) A. Dhillon, M. Nair and D. Kumar, *Anal. Methods*, 2016, **8**, 5338; (b) M. H. Arhima, O. P. Gulati and S. C. Sharma, *Phytother. Res*., 2004, **18**, 244; (c) H. Matsui, M. Morimoto and K. Horimoto, *Toxicol. In Vitro*, 2007, **21**, 1113; (d) H. S. Horowitz, *J. Public Health Dent*., 2003, **63**, 3; (e) S. Ayoob and A. K. Gupta, *Crit. Rev. Environ. Sci. Technol*., 2006, **36**, 433; (f) E. Bassin, D. Wypij, R. Davis and M. Mittleman, *Cancer Causes Control*, 2006, **17**, 421.

8 (a) J. J. Lee, G. J. Park and Y. W. Choi, *Sensors and Actuators B*., 2015, **207**, 123 ; (b) C. B. Rosen, D. J. Hansen and V. Kurt, *Org. Biomol. Chem*., 2013, **11**, 7916; (c) N. Ahmed, V. Suresh and B. Shirinfar, *Org. Biomol. Chem*., 2012, **10**, 2094; (d) G. R. You, G. J. Park and S. A. Lee, *Sensors and Actuators B*., 2014, **202**, 645.

9 E. J. Song, H. Kim and I. H. Hwang, *Sensor and Actuators B*., 2014, **195**, 36.

10 L. Y. Wang, H. H. Li and D. Cao, *Sensors and Actuators B.*, 2013, **181**, 749.

11 (a) J. L. Zhao, H. Tomiyasu and C. Wu, *Tetrahedron.*, 2015, **71**, 8521; (b) Y. S. Wu, C. Y. Li and Y. F. Li, *Sensors and Actuators B*., 2014, **203**, 712.

12 (a) J. P. E. Grolier and J. M. D. Río, *J. Chem. Thermodyn*., 2012, **55**, 193; (b) J. Makowska, K. Żamojć and D. Wyrzykowski, *Acta A*, 2016, **153**, 451; (c) E. Freire, O. L. Mayorga and M. Straume, *Anal. Chem*., 1990, **62**, 950A.

13 (a) Y. P. Zhang and S. M. Jiang, *Org. Biomol. Chem*., 2012, **10**, 6973; (b) D. Sharma, S. K. Sahoo and S. Chaudhary, *Analyst*, 2013, **138**, 3646; (c) H. Khanmohammadi and K. Rezaeian, *RSC Adv*., 2014, **4**,1032.

14 N. M. Nelly, D. D. Shihab and E. A. Edikan, *J. Incl. Phenom. Macrocycl. Chem*., 2010, **68**, 305.

15 (a)M. Orojloo and S. Amani, *Talanta.*, 2016, **159**, 292; (b) C. X. Yuan, S. Y. Li, Y. B. Wu, L. P. Lu and M.L. Zhu, *Sensors and Actuators B*., 2016, http://dx.doi.org/10.1016/j.snb.2016. 09.149; (c) A. K. Das, S.Goswami, C. K. Quah and H. K. Fun, *RSC Adv*.,2016, **6**,18711; (d) M. Nemati, R. Hosseinzadeh, R. Zadmard and M. Mohadjeranj, *Sensors and Actuators B.*, 2017, **241**, 690; (e) A. Dhara, N. Guchhait, I. Mukherjee, A. Mukherjee and S. C. Bhattacharya, *RSC Adv.*,2016, **6**, 105930.